Electronic Supplementary Material (ESI) for Journal of Materials Chemistry A.

Supporting Information

Pseudomorphic-phase transformation of NiCo based ternary hierarchical 2D-1D nanostructures for enhanced electrocatalysis

Wei Yang Lim[a], Yee-Fun Lim[b], and Ghim Wei Ho[abc]*

[a] Department of Electrical and Computer Engineering, National University of Singapore, 4 Engineering Drive 3, Singapore 117583

[b] Institute of Materials Research and Engineering, A*STAR (Agency for Science, Technology and Research), 2 Fusionopolis Way, Singapore 138634

[c] Engineering Science Programme, National University of Singapore, 9 Engineering Drive 1, Singapore 117575

Experimental Section

Reagents and chemicals

Nickel foam, Nickel nitrate ($Ni(NO_3)_2$), cobalt nitrate ($Co(NO_3)_2$), urea (CH_4N_2O), ammonium fluoride (NH_4F), sodium sulfide (Na_2S), sulfuric acid (H_2SO_4) were analytical grade and used as received without further purification.

Synthesis of 2D nanosheets-1D nanowires Nickel Cobalt hydroxide composite intermediates (NC-H)

NiCo hydroxide was prepared through the following procedures: 219 mg $Co(NO_3)_2$, 219 mg $Ni(NO_3)_2$, 148 mg NH_4F and 601 mg Urea were mixed in 25 mL of deionized water and stirred for 10 min. The precursor solution was then transferred to a Teflon-lined stainless steel autoclave of 50 mL capacity and heated at 100^{o}C for 10 h. A purple precipitate was obtained, washed with water and ethanol for three times successively, and dried for 3 h at 55^{o}C. A direct growth of same NiCo hydroxide on Ni foam was achieved using the same process, additionally with a Ni foam, sized 2 cm x 3 cm x 2 mm, submerged inside the precursor solution prior to the heating process.

Synthesis of Nickel Cobalt oxide (NC-O) and sulfide (NC-S)

The formation of NiCo oxide involved an annealing process of as-synthesized NiCo hydroxide, by heating the NC-H powder or NC-H foam at 400^{o}C for 3 h with a ramp rate of 5^{o}C/min. Black products were resulted after the annealing process. On the other hand, NiCo sulfide was formed via a sulfurization process of as-synthesized NiCo hydroxide, by placing the NC-H powder or NC-H foam into a Teflon-lined stainless steel autoclave containing 25 mL 0.1M Na_2S aqueous solution, and heating at 160^{o}C for 8 h. Black products were obtained, washed with water and ethanol for three time successively, and dried for 3h at 55^{o}C. NC-S with pure 2D nanosheets was produced in the similar course, except the heating duration was shortened to 3 h.

Characterization

Field-Emission scanning electron microscopy (FESEM, JEOL FEG JSM 7001F) operated at 15 kV was used to characterize the morphology of the synthesized catalyst. The crystallographic structures of each catalyst were analyzed using X-ray diffraction (XRD, Philips X-ray diffractometer equipped with graphite-monochromated Cu-Kα radiation at λ=1.541Å) and Transmission electron microscopy (TEM, Phillips FED CM300). X-ray photoelectron spectroscopy (XPS) spectra were obtained on a VG Thermo Escalab 220I-XL system, and all binding energies were referred to C1s peak of 284.8 eV. Diameters of evolved bubbles were measured with the assistance of Phantom Miro 3a10 Camera operated at 2900 frames per second in 1280 x 800 resolution.

Electrochemical measurements

All electrochemical measurements were carried out using an CHI6001 electrochemical workstation in a three-electrode electrochemical cell containing 0.5 M H_2SO_4 aqueous electrolyte at room temperature. Platinum foil and Ag/AgCl electrode were used as counter electrodes and

reference electrode, respectively. The synthesized catalyst-foams were directly used as the working electrode by immersing an area of 1.5 cm^2 into the electrolyte solution. Polarization curves were obtained using linear sweep voltammetry (LSV) in a potential window of 0 V to -0.6 V versus reversible hydrogen electrode (RHE) with a scan rate of 5 mV s^{-1}. Electrochemical impedance spectroscopy (EIS) measurements were conducted in the same electrochemical setup at multiple potentials from 0.1 M to 0.01 Hz with an AC potential amplitude of 5 mV. Cyclic voltammetry (CV) were also conducted in the same electrochemical setup with various scan rate in a potential window of 0 V to -0.1 V versus RHE. The anodic and cathodic current densities were then used to elaborate the capacitance current and capacitance value. To assess the stability of each catalyst-foam, a current variation with time (i-t curve) under constant voltage was scanned for 45 – 70 h 0.5 M H_2SO_4 and 1 M KOH, respectively. The applied voltages varied across different catalyst-foam and were chosen to yield an initial current density slightly larger than 10 mA cm^{-2}.

Table S1. Comparison of electrocatalytic activities of noble-metal-free HER electrocatalysts.

Materials	Morphology	Electrode	Electrolyte	Overpotential (mV) at 10mA cm^{-2}	Tafel slope ($mV\ dec^{-1}$)	Stability (cycles / hours)	Ref.
$NiCo_2S_4$	nanosheets + nanowires	Ni foam*	0.5 M H_2SO_4	155	88	60 h	This work
MoO_3/MoS_2	core/shell	FTO*	1 M H_2SO_4	≈250	50-60	10000 in 50 mV/s	2
a Co-MoS_3	film	FTO*	0.5 M H_2SO_4	≈185	43	-	3
Cu_2MoS_4	-	glassy carbon	0.5 M H_2SO_4	≈310	95	-	4
MoS_2	film	FTO*	0.5 M H_2SO_4	≈230	50	-	5
$CoMoS_x$	film	FTO*	phosphate buffer	≈240	85	2 h	6
$CoWS_x$				≈270	78		
$NiWS_x$				≈365	96		
$Fe_{0.43}Co_{0.57}S_2$	film	glassy carbon*	0.5 M H_2SO_4	185	56	1000 in 50 mV/s	7
$CoSe_2$	film			≈230	42.4		
Ni_2P	nanoparticles	Ti foil	0.5 M H_2SO_4	120	46	500 in 100 mV/s	8
a Co-S	film	FTO*	1 M phosphate buffer	≈165	93	40 h	9
O-doped MoS_2	nanosheets	glass carbon	0.5 M H_2SO_4	≈180	55	3000 in 50 mV/s	10
$Co_{0.6}Mo_{1.4}N_2$	aggregated nanoparticles	glassy carbon	0.1 M $HClO_4$	≈200	-	-	11
1T-WS_2	exfoliated nanosheets	glass carbon	0.5 M H_2SO_4	≈260	55	120 h	12
$MoSe_2$	porous film	glassy carbon	0.1 M H_2SO_4	250	80	48 h	13
$Ni_{12}P_5$	nanoparticles	Ti foil	0.5 M H_2SO_4	107	63	≈3 h	14
$WSe_{0.96}S_{1.04}$	nanotubes	carbon fiber*	1 M H_2SO_4	≈260	105	≈2 h	15
FeP	hollow nanoparticles	Ti foil	0.5 M H_2SO_4	50	37	16 h	16
CoP	hollow nanoparticles	Ti foil	0.5 M H_2SO_4	≈75	50	24 h	17
WS_2	nanoflakes	glassy carbon	0.5 M H2SO4	≈420	48	10000 in 10 mV/s	18

Cu_3P	nanowires array	Cu foam	0.5 M H_2SO_4	143	67	3000 in 100 mV/s	19
FeP	nanowires array	Ti plate	0.5 M H_2SO_4	55	38	3000 in 100 mV/s	20
MoN	nanosheets	glassy carbon	0.5 M H_2SO_4	≈225	90	3000 in 50 mV/s	21
1T-WS_2	nanosheets	graphite	0.5 M H_2SO_4	148	70	≈4 h	22
MoP	bulk	glassy carbon	0.5 M H_2SO_4	≈135	54	40 h	23
$CoSe_2$	nanoparticles	carbon fiber*	0.5 M H_2SO_4	137	42.1	60 h	24
CoP	nanowires array	carbon fiber*	0.5 M H_2SO_4 1 M KOH	67 209	51 129	5000 in 100 mV/s -	25
CoS_2	microwires array	glassy carbon	0.5 M H_2SO_4	145	51.4	40 h	26
Co_2P	nanorods	Ti foil	0.5 M H_2SO_4	134	51.7	12 h	27
Co_9S_8/C	core/shell	glassy carbon	0.5 M H_2SO_4 1 M KOH 1 M phosphate buffer	240 250 280	-	10 h	28
CoP/$CoPO_4$	film	glass, Si, Fe*	0.5 M H_2SO_4	≈150	53	≈14 h	29
Co_9S_8/MoS_2	core/shell	carbon fiber*	0.5 M H_2SO_4	190	110	12 h	30
NiS	cubic nanoframes	Ni foam	1 M KOH	94	139	16 h	31
WO2/C	mesoporous nanowires	glassy carbon	0.5 M H_2SO_4	58	46	10 h	32
Ni_3S_2	nanosheets array	Ni foam*	neutral 1 M NaOH	170 223	-	200 h 150 h	33
α-Fe-Ni-S	nanosheets	glassy carbon	0.5 M H_2SO_4	105	40	39 h	34
NiS	rod-shaped nanoparticles	glassy carbon	0.5 M H_2SO_4	≈260	88	5000 in 50 mV/s	35
MoS_2/$CoSe_2$	nanosheets/nanobelts	glassy carbon	0.5 M H_2SO_4	≈75	36	24 h	36
$WO_{2.9}$	nanoparticles	glassy carbon	0.5 M H_2SO_4	70	50	10000 in 5 mV/s	37
Ni-Mo-S	nanosheets	carbon fiber*	0.5 M phosphate buffer	200	85.3	≈8 h	38
NiFe/$NiCo_2O_4$	nanosheets/nanoflakes	Ni foam*	1 M KOH	105	88	10 h	39
$NiCo_2S_4$	nanowires array	Ni foam*	1 M KOH	210	58.9	50 h	40

NiS	microspheres	Ni foam*	1 M KOH	158	83	20 h	41
$Zn_{0.3}Co_{2.7}S_4$	hollow framework	-	0.5 M H_2SO_4	80	47.5	60 h	42
Ni_3S_2	leaves	Ni foam*	1 M KOH	182	89	12 h	43

*direct assembly on electrode

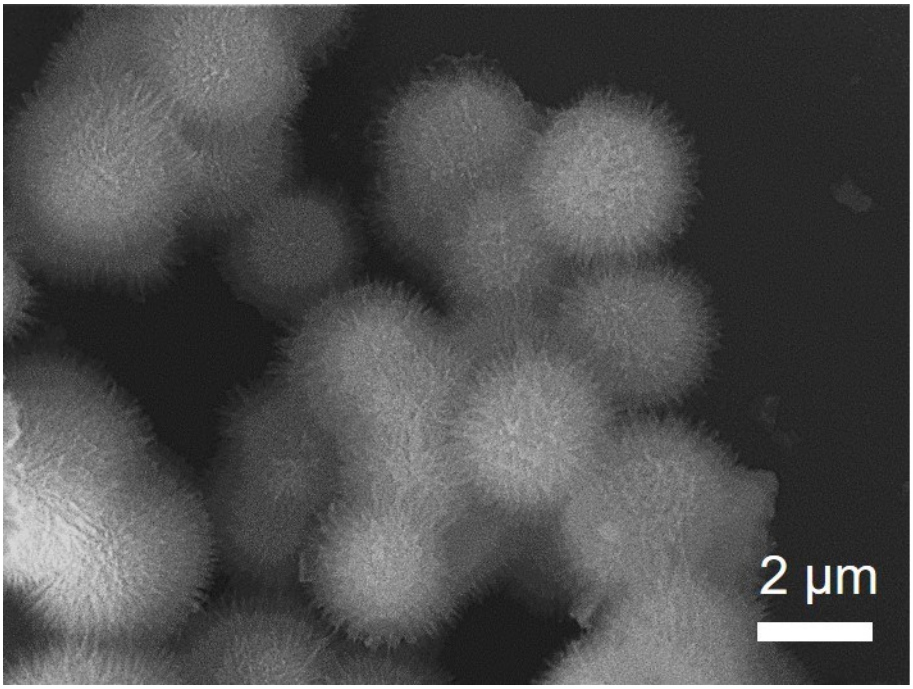

Figure S1. SEM image of self-assembled microspheres with 1D nanowires NiCo-$(OH)_2$ synthesized without the presence of ammonium fluoride.

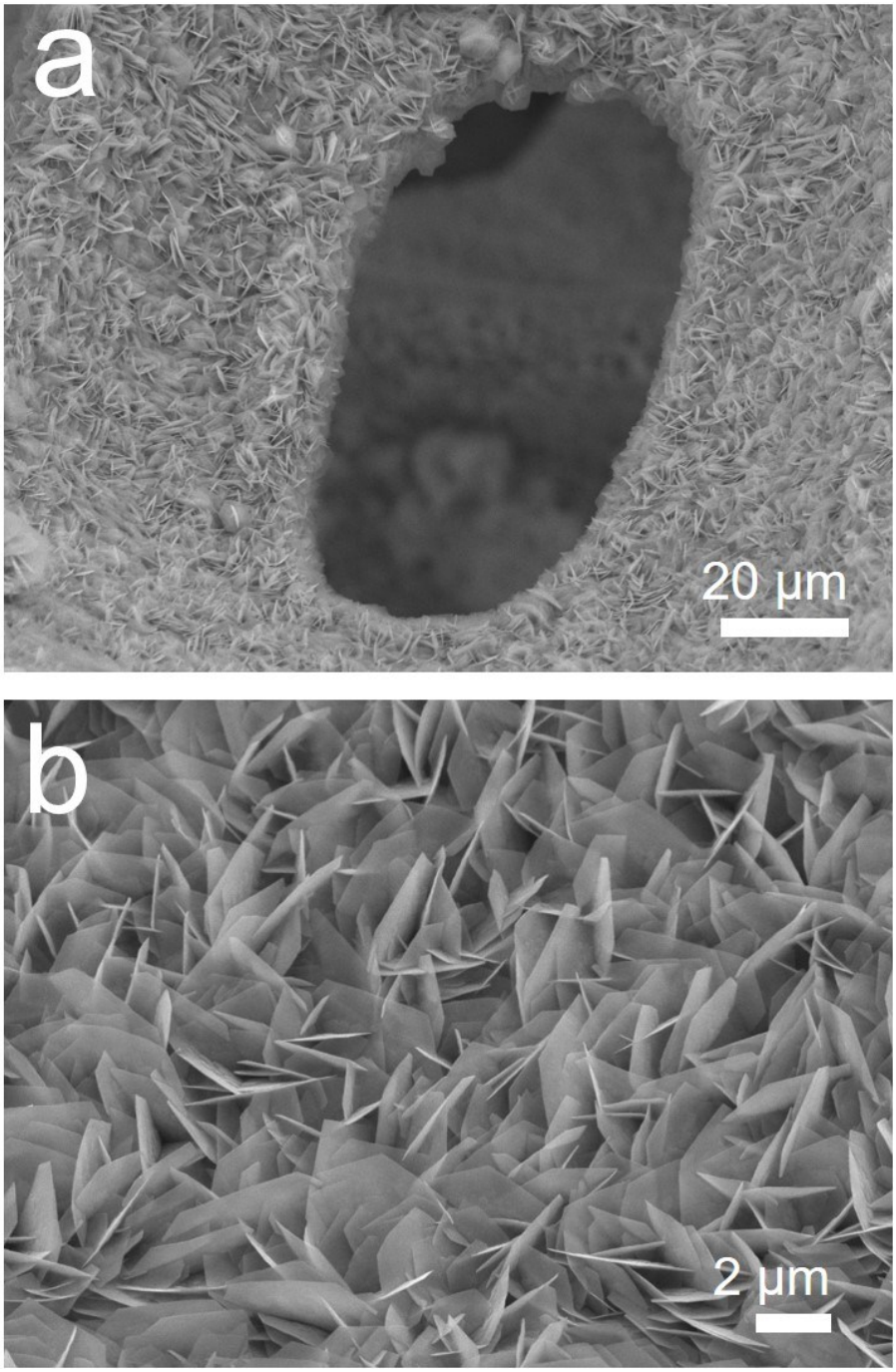

Figure S2. SEM images in (a) low magnification and (b) high magnification of Nickel Cobalt hydroxides directly grown on nickel foam at growth duration of 3 h.

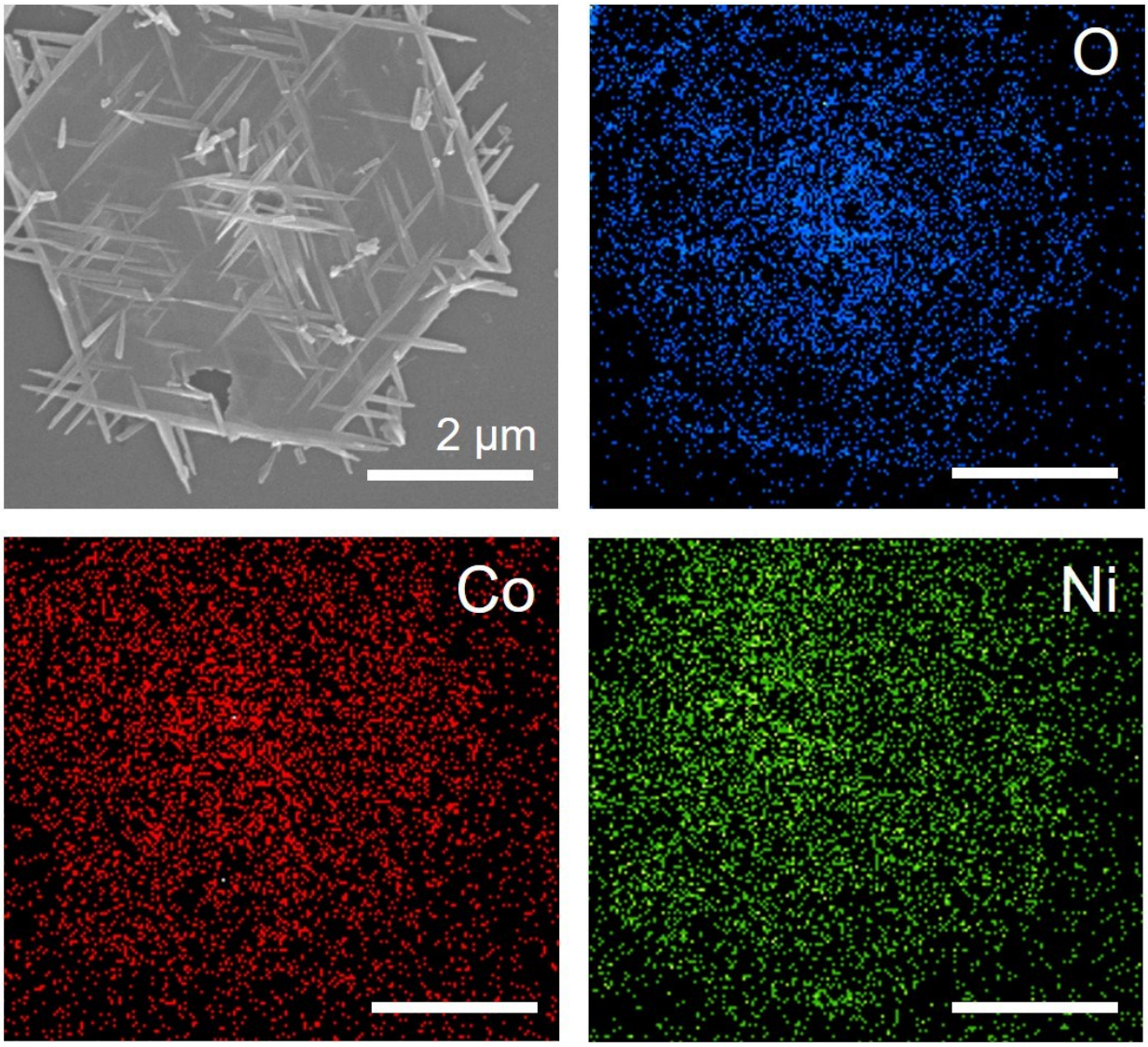

Figure S3. Energy Dispersive X-ray (EDX) mapping of uniformly distributed Co, Ni and O elements of NC-H.

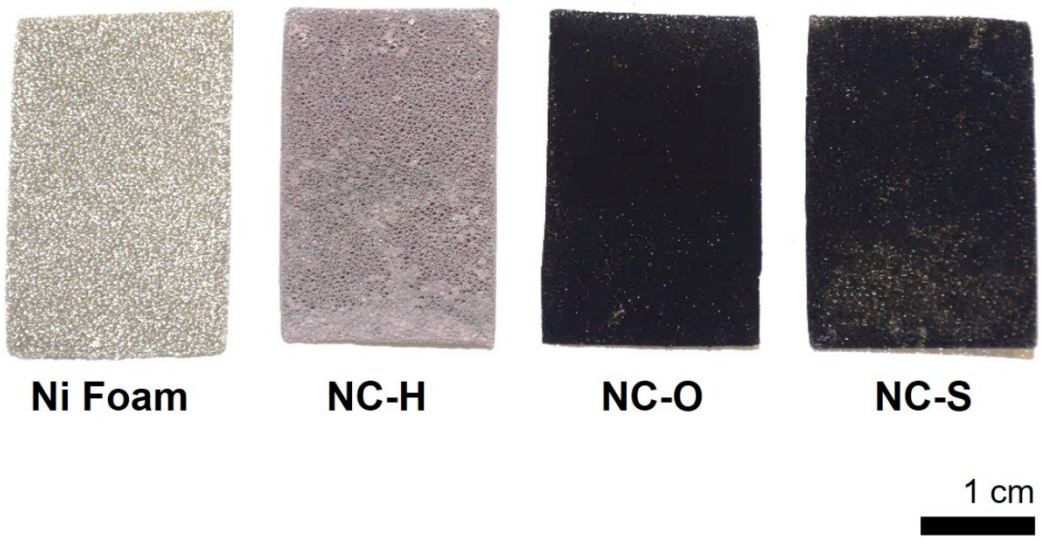

Figure S4. Digital photos of nickel foam and nickel foam grown with NC-H, NC-O and NC-S, respectively.

The Ni 2p XPS spectra Ni 2p peaks split into Ni $2p_{3/2}$ (855.6 eV) and Ni $2p_{1/2}$ (873.1 eV), accompanied by satellite lines at 861.6 eV and 879.9 eV respectively; Co 2p peaks split into Co $2p_{3/2}$ (781.3 eV) and Co $2p_{1/2}$ (797.4 eV), accompanied by satellite lines at 785.9 eV and 803.1 eV respectively.

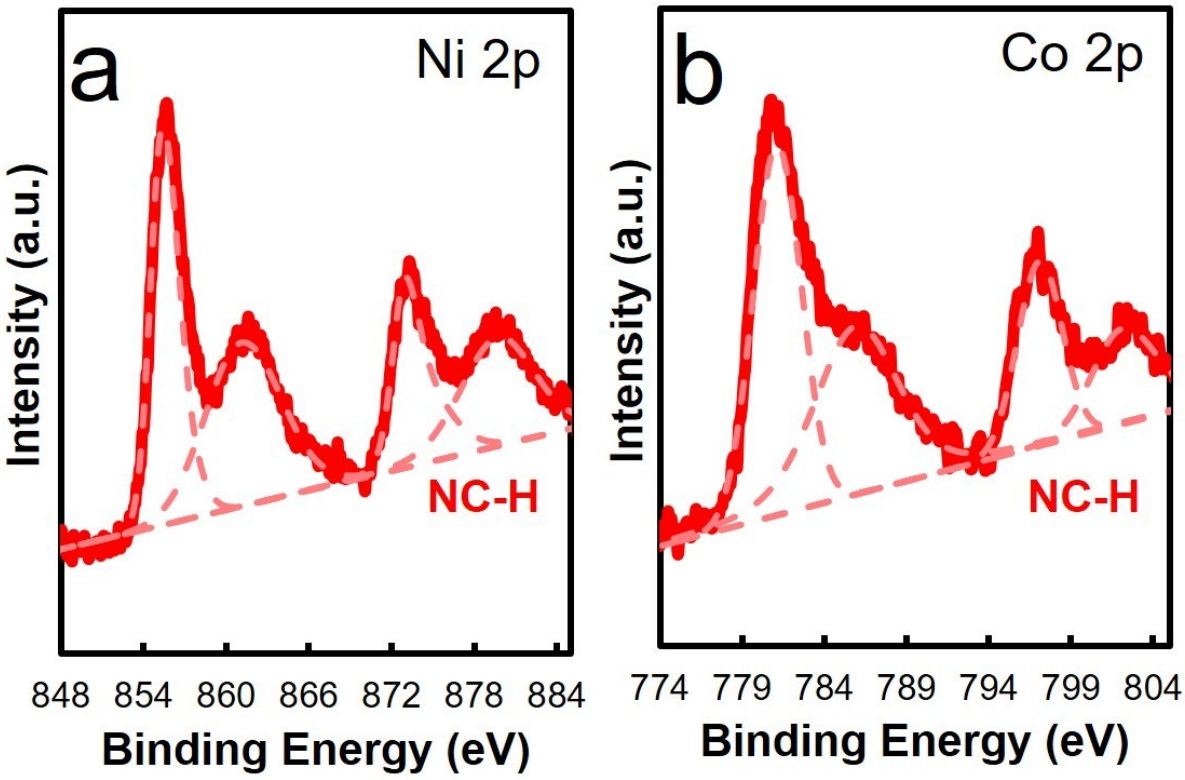

Figure S5. XPS spectra of NC-H on (a) Ni 2p core and (b) Co 2p core levels.

The Co 2p XPS spectrum shows two spin-orbit doublets: the binding energies at 778.8 eV for Co $2p_{1/2}$ and 793.7 eV for Co $2p_{3/2}$ with spin-orbiting splitting values of 15.1eV are spin-orbit characteristic of Co^{3+}, while the binding energies at 781.6 eV for Co $2p_{1/2}$ and 797.3 eV for Co $2p_{3/2}$ with spin-orbiting splitting value of 16.3 eV are spin-orbit characteristic of Co^{2+}. The weak satellite peaks indicate that the majority of Co atoms were in the Co^{3+} state.

The Ni 2p XPS spectrum shows two spin-orbit doublets: the binding energies at 853.2 eV for Ni $2p_{3/2}$ and 872.6 eV for Ni $2p_{1/2}$ are spin-orbit characteristics of Ni^{2+}, while the binding energies at 856.2 eV for Ni $2p_{3/2}$ and 874.4 eV for Ni $2p_{1/2}$ are spin-orbit characteristics of Ni^{3+}. Likewise, an intense satellite peak suggested that the Ni state was predominant in the Ni^{2+} state.[1]

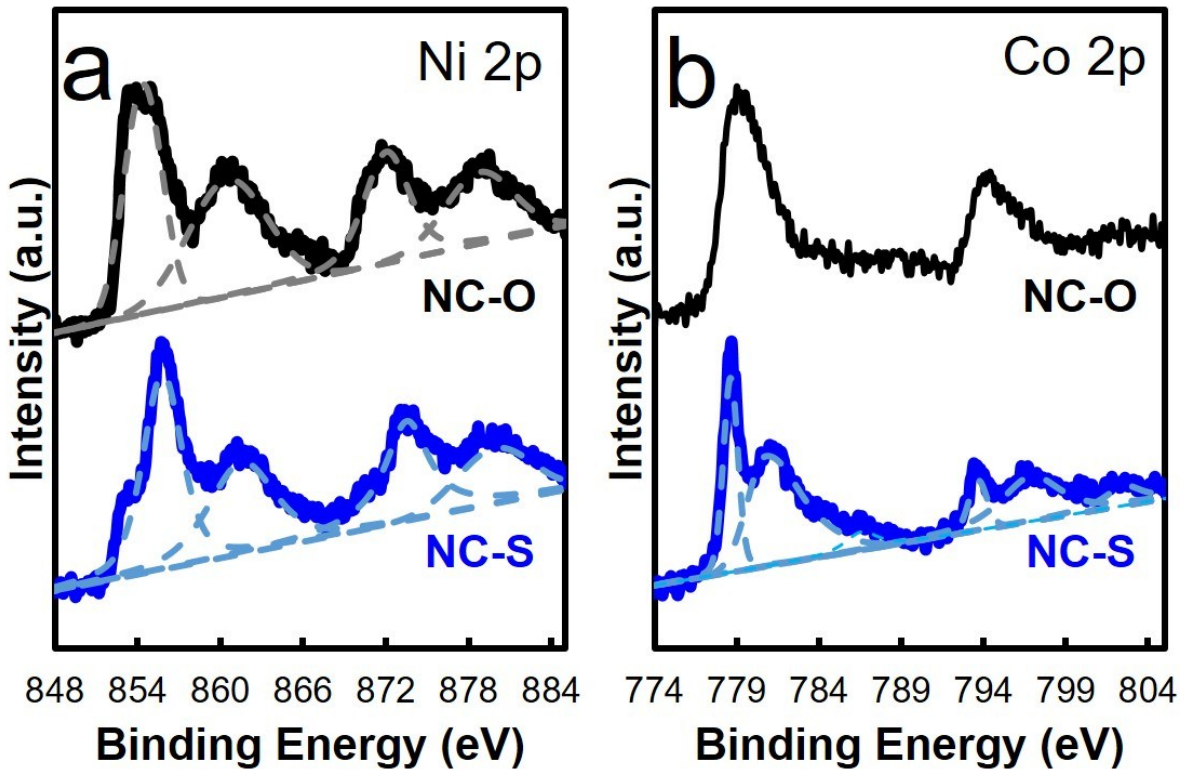

Figure S6. XPS spectra of NC-O and NC-S on (a) Ni 2p and (b) Co 2p core levels.

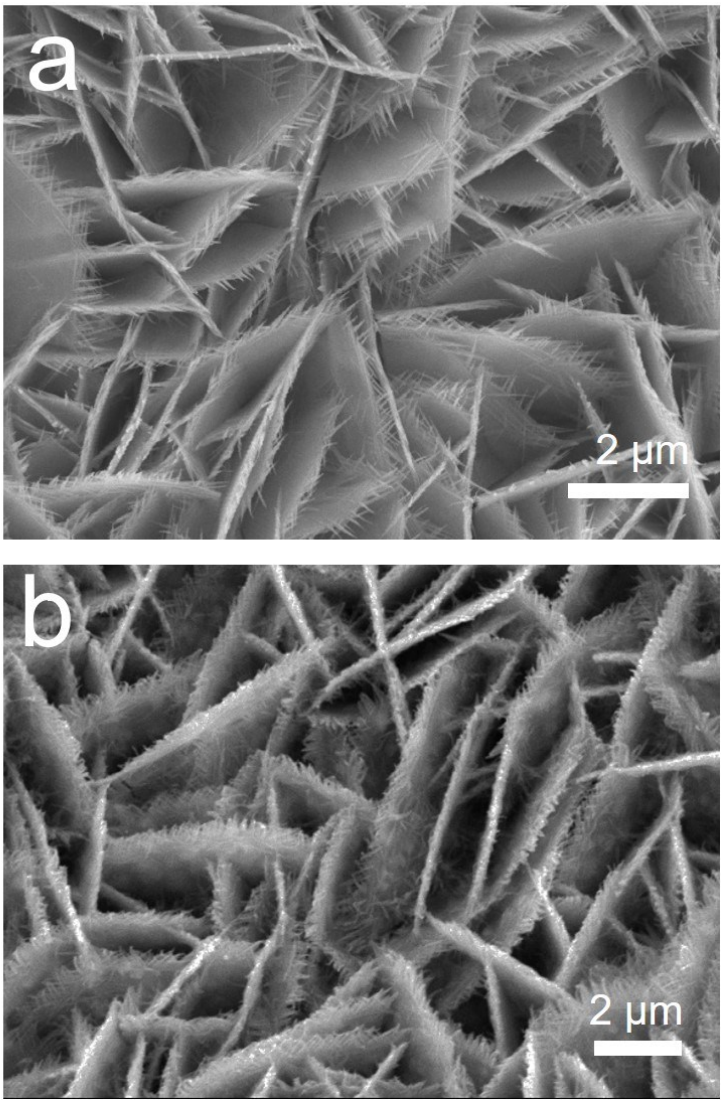

Figure S7. SEM images of (a) NC-O and (b) NC-S directly grown on nickel foam.

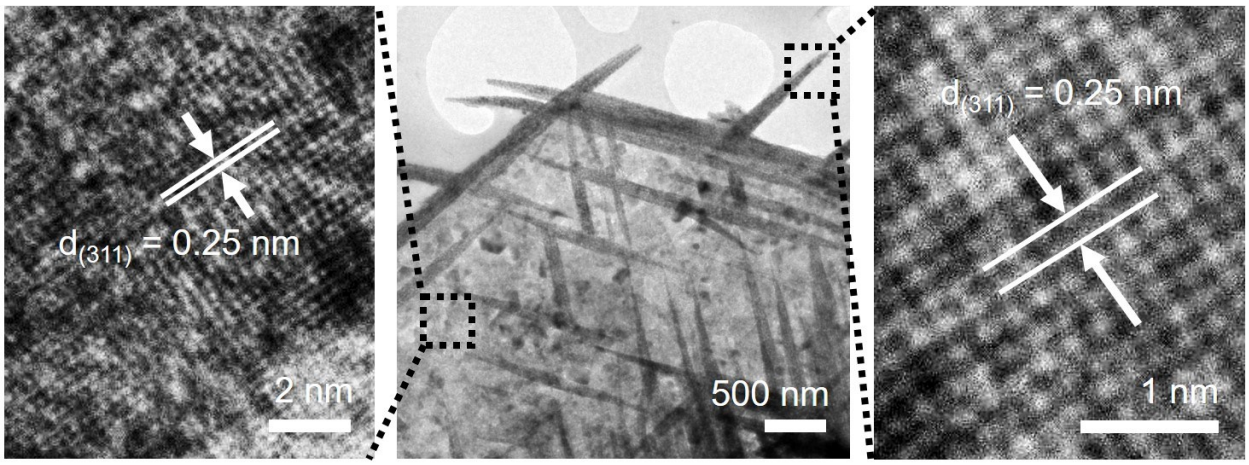

Figure S8. TEM images of NC-O and HRTEM images of nanosheets and nanowires, showing clear crystal fringes with 0.25 nm spacing, corresponding to interplanar distance of (311) plane of $NiCo_2O_4$.

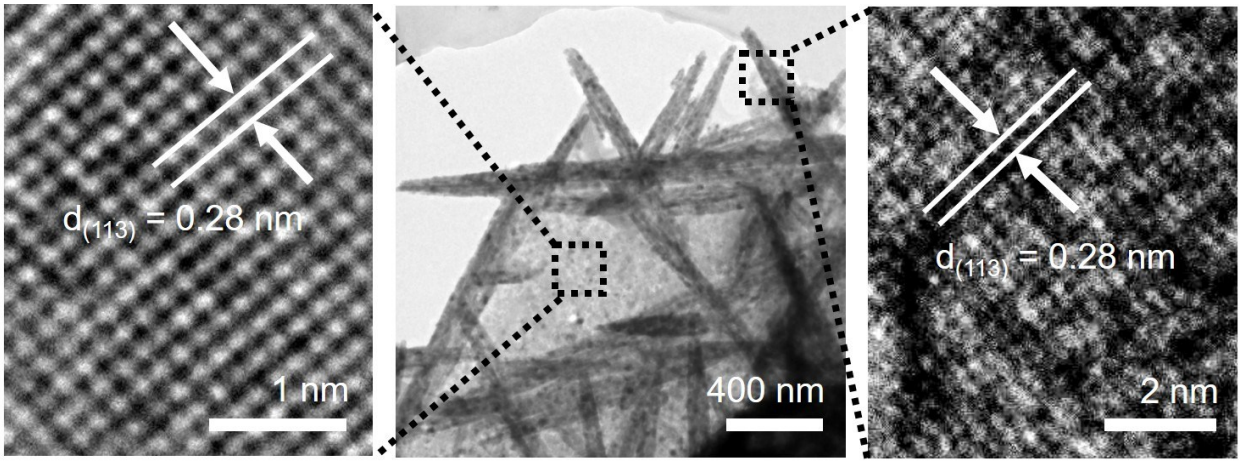

Figure S9. TEM images of NC-S and HRTEM images of nanosheets and nanowires, showing clear crystal fringes with 0.28 nm spacing, corresponding to interplanar distance of (113) plane of $NiCo_2S_4$.

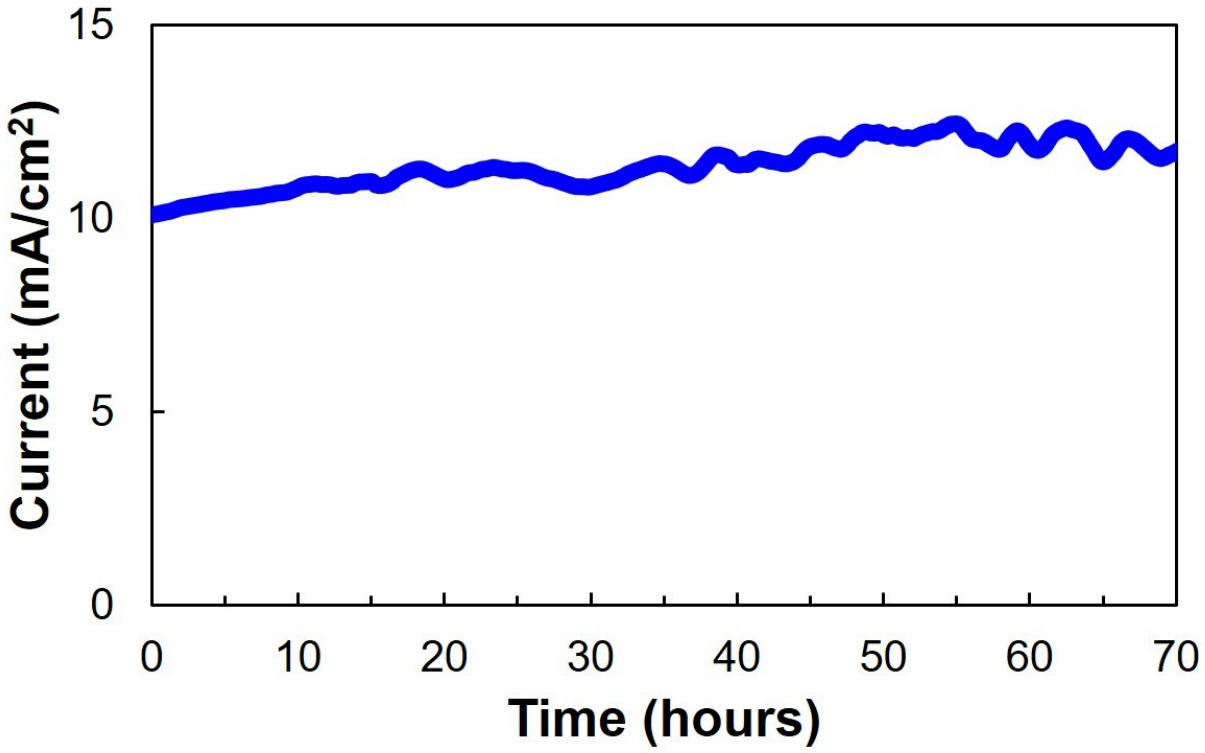

Figure S10. Chronoamperometry test (i-t curve) of NC-S in acidic electrolyte of 0.5 M H_2SO_4 at current density of 10 mA cm^{-2} up to 60 h for stability assessment.

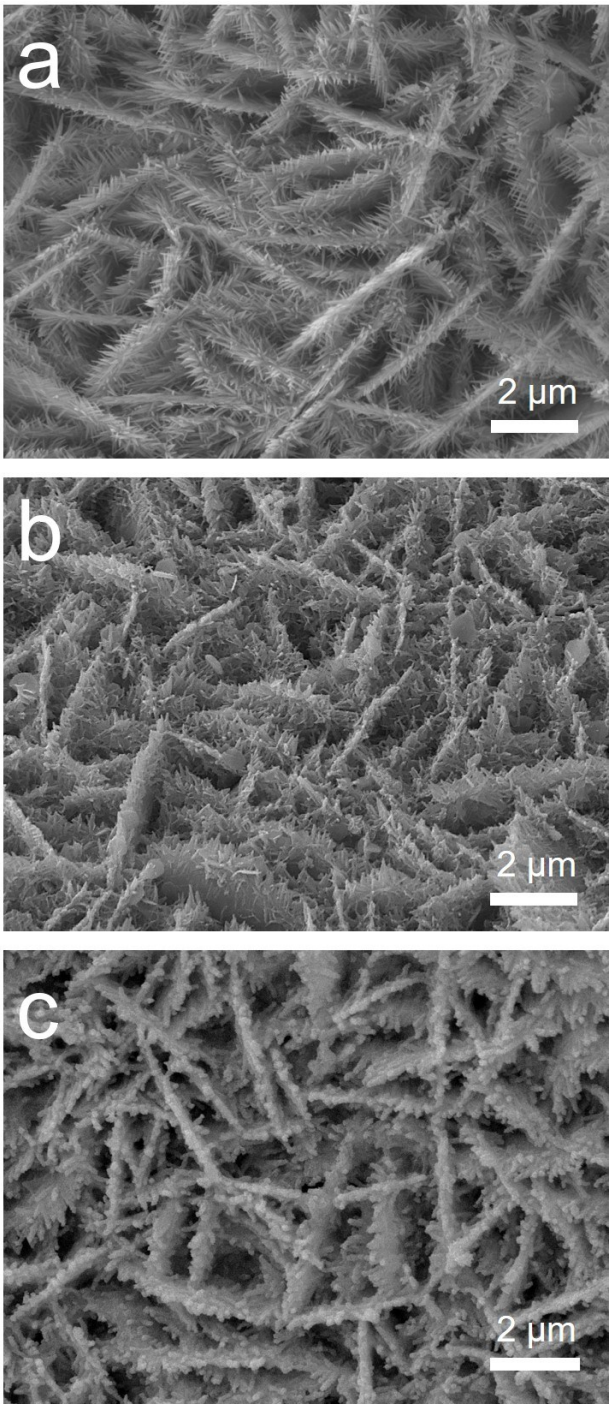

Figure S11. SEM images of (a) NC-H, (b) NC-O and (c) NC-S on Ni foam after a chronoamperometry test for stability assessment.

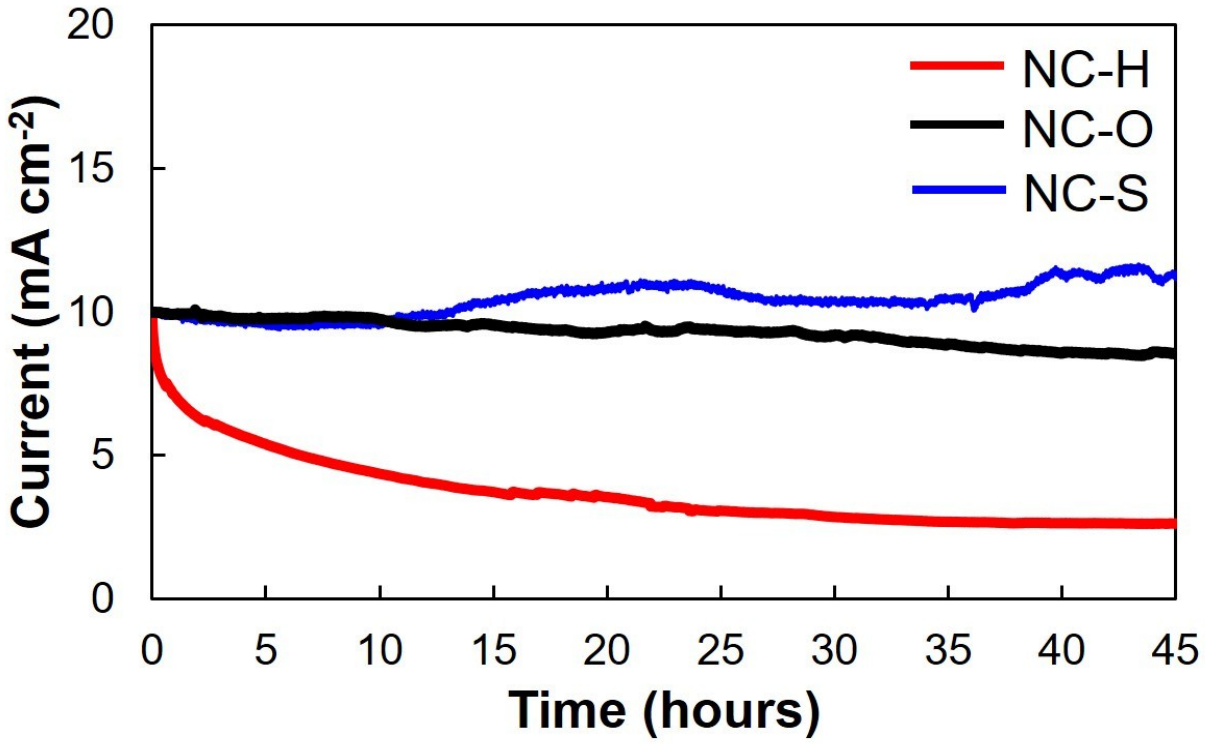

Figure S12. Chronoamperometry test (i-t curve) of NC-H, NC-O and NC-S in basic electrolyte of 1 M KOH at current density of 10 mA cm^{-2} up to 45 h for stability assessment.

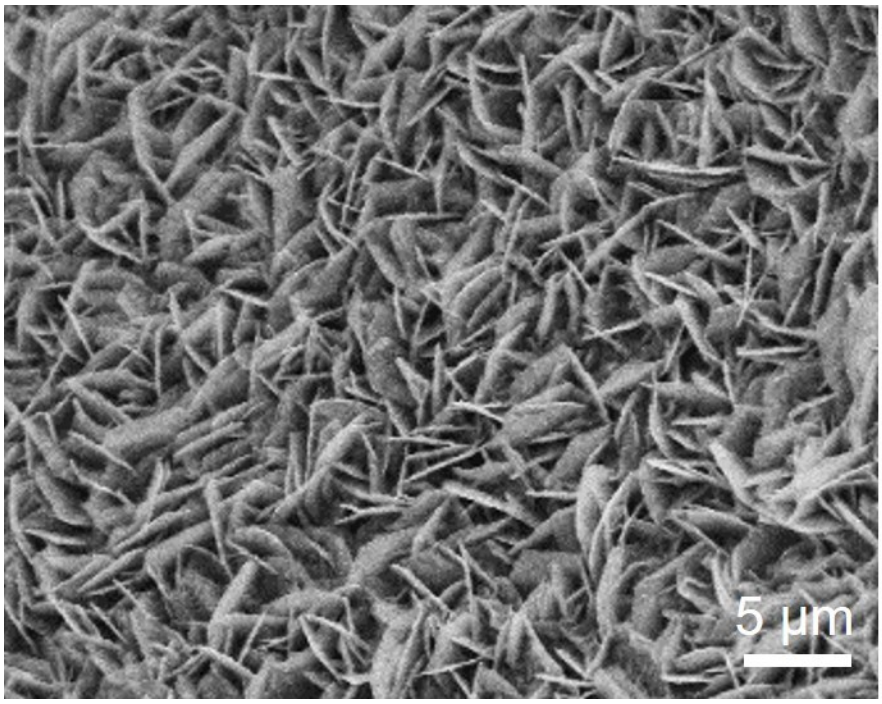

Figure S13. SEM images of NC-S2 (Nickel Cobalt sulfide with 2D nanosheets, transformed from Nickel Cobalt hydroxides directly grown on nickel foam at growth duration of 3 h, sees Figure S2).

Reference

1 A. Sivanantham, P. Ganesan, S. Shanmugam, Adv. Funct. Mater., 2016, **26**, 4661-4672.

2 Z. Chen., D. Cummins, B. N. Reinecke, E. Clark, M. K. Sunkara, T. F. Jaramillo, Nano Lett., 2011, 11, 4168-4175

3 D. Merki, H. Vrubel, L. Rovelli, S. Fierro, X. Hu, Chem. Sci., 2012, 3, 2515-2525

4 P. D. Tran, M. Nguyen, S. S. Pramana, A. Bhattacharjee, S. Y. Chiam, J. Fize, M. J. Field, V. Artero, L. H. Wong, J. Loo, J. Barber, Energy Environ. Sci., 2012, 5, 8912-8916,

5 J. Kibsgaard, Z. Chen, B. N. Reinecke, T. F. Jaramillo, Nat. Mater., 2012, 963-969

6 P. D. Tran , S. Y. Chiam, P. P. Boix, Y. Ren, S. S. Pramana, J. Fize, V. Artero, J. Barber, Energy Environ. Sci., 2013, 6, 2452-2459

7 D. Kong, J. J. Cha, H. Wang, H. R. Lee, Y. Cui, Energy Environ. Sci., 2013, 6, 3553-3558

8 E. J. Popczun, J. R. Mckone, C. G. Read, A. J. Biacchi, A. M. Wiltrout, N. S. Lewis, R. E. Schaak, J. Am. Chem. Soc., 2013, 135, 9267-9270

9 Y. Sun, C. Liu, D. C. Grauer, J. Yano, J. R. Long, P. Yang, C. J. Chang, J. Am. Chem. Soc., 2013, 135, 17699-17702

10 J. Xie, J. Zhang, S. Li, F. Grote, X. Zhang, H. Zhang, R. Wang, Y. Lei, B. Pan, Y. Xie, J. Am. Chem. Soc., 2013, 135, 17881-17888

11 B. Cao, G. M. Veith, J. C. Neuefeind, R. R. Adzic, P. G. Khalifah, J. Am. Chem. Soc., 2013, 135, 19186-19192

12 D. Voiry, H. Yamaguchi, J. Li, R. Silva, D. C. B. Alves, T. Fujita, M. Chen, T. Asefa, V. B. Shenoy, G. Eda, M. Chhowalla, Nat. Mater., 2013, 12, 850-855

13 F. H. Saadi, A. I. Carim, J. M. Velazquez, J. H. Baricuatro, C. C. L. McCrory, M. P. Soriaga, N. S. Lewis, ACS Catal., 2014, 4, 2866-2873

14 Z. Huang, Z. Chen, Z. Chen, C. Lv, H. Meng, C. Zhang, ACS Nano, 2014, 8, 8121-8129

15 K. Xu, F. Wang, Z. Wang, X. Zhan, Q. Wang, Z. Cheng, M. Safdar, J. He, ACS Nano, 2014, 8, 8468-8476

16 J. F. Callejas, J. M. McEnaney, C. G. Read, J. C. Crompton, A. J. Biacchi, E. J. Popczun, T. R. Gordon, N. S. Lewis, R. E. Schaak, ACS Nano, 2014, 8, 11101-11107

17 E. J. Popczun, C. G. Read, C. W. Roske, N. S. Lewis, Y. E. Schaak, Angew. Chem. Int. Ed., 2014, 53, 5427-5430

18 L. Cheng, W. Huang, Q. Gong, C. Liu, Z. Liu, Y. Li, H. Dai, Angew. Chem. Int. Ed., 2014, 53, 7860-7863

19 J. Tian, Q. Liu, N. Cheng, A. M. Asiri, Angew. Chem. Int. Ed., 2014, 53, 9577-9581

20 P. Jiang, Q. Liu, Y. Liang, J. Tian, A. M. Asiri, X. Sun, Angew. Chem. Int. Ed., 2014, 53, 12855-12859

21 J. Xie, S. Li, X. Zhang, J. Zhang, R. Wang, H. Zhang, B. Pan, Y. Xie, Chem. Sci., 2014, 5, 4615-4620

22 M. A. Lukowski, A. S. Daniel, C. R. English, F. Meng, A. Forticaux, R. J. Hamers, S. Jin, Energy Environ. Sci., 2014, 7, 2608-2613

23 P. Xiao, M. A. Sk, L. Thia, X. Ge, R. J. Lim, J.-Y. Wang, K. H. Lim, X. Wang, Energy Environ. Sci., 2014, 7, 2624-2629

24 D. Kong, H. Wang, Z. Lu, Y. Cui, J. Am. Chem. Soc., 2014, 136, 4897-4900

25 J. Tian, Q. Liu, A. M. Asiri, X. Sun, J. Am. Chem. Soc., 2014, 136, 7587-7590
26 M. S. Faber, R. Dziedzic, M. A. Lukowski, N. S. Kaiser, Q. Ding, S. Jin, J. Am. Chem. Soc., 2014, 136, 10053-10061
27 Z. Huang, Z. Chen, Z. Chen, C. Lv, M. G. Humphrey, C. Zhang, Nano Energy, 2014, 9, 373-382
28 L.-L. Feng, G.-D. Li, Y. Liu, Y. Wu, H. Chen, Y. Wang, Y.-C. Zou, D. Wang, X. Zou, ACS Appl. Mater. Interfaces, 2015, 7, 980-988
29 Y. Yang, H. Fei, G. Ruan, J. M. Tour, Adv. Mater., 2015, 27, 3175-3180
30 H. Zhu, J. Zhang, R. Yanzhang, M. Du, Q. Wang, G. Gao, J. Wu, G. Wu, M. Zhang, B. Liu, J. Yao, X. Zhang, Adv. Mater., 2015, 27, 4752-4759
31 X.-Y. Yu, L. Yu, H. B. Wu, X. W. Lou, Angew. Chem. Int. Ed., 2015, 54, 5331-5335
32 R. Wu, J. Zhang, Y. Shi, D. Liu, B. Zhang, J. Am. Chem. Soc., 2015, 137, 6983-6986
33 L.-L. Feng, G. Yu, Y. Wu, G.-D. Li, H. Li, Y. Sun, T. Asefa, W. Chen, X. Zou, J. Am. Chem. Soc., 2015, 137, 14023-14026
34 M. D. Greengalgh, S. P. Thomas, J. Am. Chem. Soc., 2015, 138, 11900-11903
35 D. Y. Chung, J. W. Han, D.-H. Lim, J.-H. Jo, S. J. Yoo, H. Lee, Y.-E. Sung, Nanoscale, 2015, 7, 5157-5163
36 M.-R. Gao, J.-X. Liang, Y.-R. Zheng, Y.-F. Xu, J. Jiang, Q. Gao, J. li, S.-H. Yu, Nat. Commun., 2015, 6, 5982
37 Z.-F. Huang, J. Song, K. Li, M. Tahir, Y.-T. Wang, L. Pan, L. Wang, X. Zhang, J.-J. Zou, Nat. Commun., 2015, 6, 8064
38 J. Miao, F.-X. Xiao, H. B. Yang, S. Y. Khoo, J. Chen, Z. Fan, Y.-Y. Hsu, H. M. Chen, H. Zhang, B. Liu, Sci. Adv., 2015, 1:e1500259
39 C. Xiao, Y. Li, X. Lu, C. Zhao, Adv. Funct. Mater., 2016, 26, 3515-3523
40 A. Sivanantham, P. Ganesan, S. Shanmugam, Adv. Funct. Mater., 2016, 26, 4661-4672
41 W. Zhu, X. Yue, W. Zhang, S. Yu, Y. Zhang, J. Wang, J. Wang, Chem. Commun., 2016, 52, 1486-1489
42 Z.-F. Huang, J. Song, K. Li, M. Tahir, Y.-T. Wang, L. Pan, L. Wang, X. Zhang, J.-J. Zou, J. Am. Chem. Soc., 2016, 138, 1359-1365
43 T. Zhu, L. Zhu, J. Wang, G. W. Ho, J. Mater. Chem. A., 2016, 4, 13916-13922